

Short Communication

## Synthesis of Single-Crystalline Iron Oxide Magnetic Nanorings as Electrochemical Biosensor for Dopamine Detection

Xiaonan Liu<sup>1,3</sup>, Fanghua Zhu<sup>2</sup>, Wei Wang<sup>3</sup>, Jiehong Lei<sup>4</sup>, Guangfu Yin<sup>1,\*</sup>

<sup>1</sup> College of Materials Science and Engineering, Sichuan University, Sichuan 610064, P. R. China

<sup>2</sup> Research Center of Laser Fusion, China Academy of Engineering Physics, Mianyang, Sichuan 621900, China

<sup>3</sup> School of Materials Science and Engineering, Southwest University of Science and Technology, Mianyang, 621010, China

<sup>4</sup> College of Physics and Space Science, China West Normal University, Nanchong 637009, China.

\*E-mail: [nic0700@scu.edu.cn](mailto:nic0700@scu.edu.cn)

Received: 13 August 2016 / Accepted: 17 September 2016 / Published: 10 October 2016

---

In this paper, uniform iron oxide magnetic nanorings (Fe<sub>3</sub>O<sub>4</sub> NRs) were successfully synthesized through hydrothermal method. The electrochemical performance of Fe<sub>3</sub>O<sub>4</sub> NRs/glassy carbon electrode (GCE) based biosensor for dopamine (DA) detection has been investigated by cyclic voltammetry (CV) and differential pulse voltammetry (DPV). These results implied the Fe<sub>3</sub>O<sub>4</sub> NRs/GCE biosensor exhibited superior electrocatalytic activity and significant electron transfer kinetics for the electrooxidation of DA with a quick response time of 4 s and a low detection limit of 10 nM. These excellent electrochemical results indicate the Fe<sub>3</sub>O<sub>4</sub> NRs could be utilized as an extremely promising material for the detection of DA related diseases in biomedical analysis.

---

**Keywords:** Fe<sub>3</sub>O<sub>4</sub> nanorings, dopamine, electrooxidation, cyclic voltammetry

### 1. INTRODUCTION

Recently, the application of nanomaterials modified electrodes in electrochemical biosensor has received much attention [1-3]. In these electrodes, magnetic nanomaterials based electrochemical biosensors exhibits excellent properties, because of their high sensitivity, fast response speed, good selectivity, high specific surface area and good electrical conductivity [4-7].

The magnetic nanomaterials modified electrode or incorporated into the electrode can significantly increase the surface area, and accelerate electron transfer. It is possible to improve the electrode stability, accelerate the response speed, and enhance the selectivity of detection [8].

Dopamine (DA) is considered as one of the most momentous and representative of catecholamine neurotransmitter, which is one of the most important transmission media of mammalian and human important central nervous system [9]. The restricting of DA transmission is likely to cause neurological disorders, such as schizophrenia, Alzheimer's and Parkinson's diseases. Therefore, detection of the changes of DA concentrations can prevent a variety of diseases, so fast, highly sensitive and accurate measurement of dopamine is very important. At present, there are many methods to detect DA concentration, such as fluorescence, liquid chromatography and chemiluminescence methods. Because dopamine is prone to electrochemical oxidation, the electrochemical sensor of DA detection has many advantages, such as higher accuracy, faster response and lower cost [10].

Wang *et al.* [11] prepared magnetic Fe<sub>3</sub>O<sub>4</sub> hybrid nanocomposites then modified them on the glassy carbon electrode (GCE) to generate an electrochemical sensor in phosphate buffer solution (PBS) for dopamine detection. And the detection limit is  $6.67 \times 10^{-10}$  M. Peik-See *et al.* [12] described an Fe<sub>3</sub>O<sub>4</sub>/graphene modified GCE electrode as an electrochemical biosensor, where the limits of detection were 0.42 and 0.12  $\mu$ M for ascorbic acid and dopamine, respectively. Zhang *et al.* [13] prepared nafion covered core-shell structured Fe<sub>3</sub>O<sub>4</sub>@graphene nanospheres modified GCE, with a detection limit of 0.007 mM.

In the present study, we fabricated high-quality single-crystal Fe<sub>3</sub>O<sub>4</sub> nanorings (NRs), and coated them on the surface of GCE for the simultaneous electrochemical determination of DA. The Fe<sub>3</sub>O<sub>4</sub> NRs biosensor shows a high sensitivity and selectivity with a wide linear range between 0.01 and 1 mM, and a lower detection limit of 10 nM.

## 2. EXPERIMENTAL

### 2.1. Preparation of electrode materials

The uniform Fe<sub>3</sub>O<sub>4</sub> NRs were prepared by a hydrothermal method according to Jia *et al.* [14]. In a typical procedure, FeCl<sub>3</sub>, NaH<sub>2</sub>PO<sub>4</sub>, and Na<sub>2</sub>SO<sub>4</sub> aqueous solutions were mixed in 80 mL distilled water and their concentrations were controlled as 0.02,  $1.8 \times 10^{-4}$ , and  $5.5 \times 10^{-4}$  mol L<sup>-1</sup>, respectively. After that, the mixture was reacted at 220 °C for 48 h. After cooling to room temperature, the Fe<sub>3</sub>O<sub>4</sub> NRs precipitates were separated and washed with distilled water and absolute ethanol at least 3 times. Finally, the precipitates were dried under vacuum at 80 °C for 24 h.

1 mg of Fe<sub>3</sub>O<sub>4</sub> NRs was dispersed in 5 mL of dimethyl formamide (DMF), and then the suspension was prepared by ultrasonic dispersion for 30 min. After that, the bare GCE was polished to a mirror-like surface with  $\alpha$ -Al<sub>2</sub>O<sub>3</sub>. Subsequently, the bare GCE was rinsed ultrasonically with ethanol for surface cleaning. Then, 5  $\mu$ L of Fe<sub>3</sub>O<sub>4</sub> NRs were coated on GCE surface by evaporation. Finally, the Fe<sub>3</sub>O<sub>4</sub> NRs modified GCE electrode was obtained after dried under vacuum at 40 °C for 120 min.

## 2.2. Materials characterization

The morphology and microstructure of the products were characterized by field emission scanning electron microscopy (FSEM, Ultra 55) and transmission electron microscopy (TEM, 200FE Libra). The crystal structure was determined by X-ray diffraction (X'Pert, PRO XRD). The hysteresis loop of the  $\text{Fe}_3\text{O}_4$  NRs was characterized on a PPMS-9T instrument at 300K.

## 2.3. Electrochemical characterizations

The electrochemical measurements of the  $\text{Fe}_3\text{O}_4$  NRs/GCE electrodes were carried out with cyclic scan in the potential range from -1.0 to 0.8 V in 0.1 M PBS (pH 5.0) The electrochemical sensing test of the  $\text{Fe}_3\text{O}_4$  NRs/GCE electrode was performed with a electrochemistry workstation (IM6, Germany) by a conventional three-electrode system, and then differential-pulse voltammetry (DPV) and cyclic voltammetry (CV) results were recorded.

## 3. RESULTS AND DISCUSSION

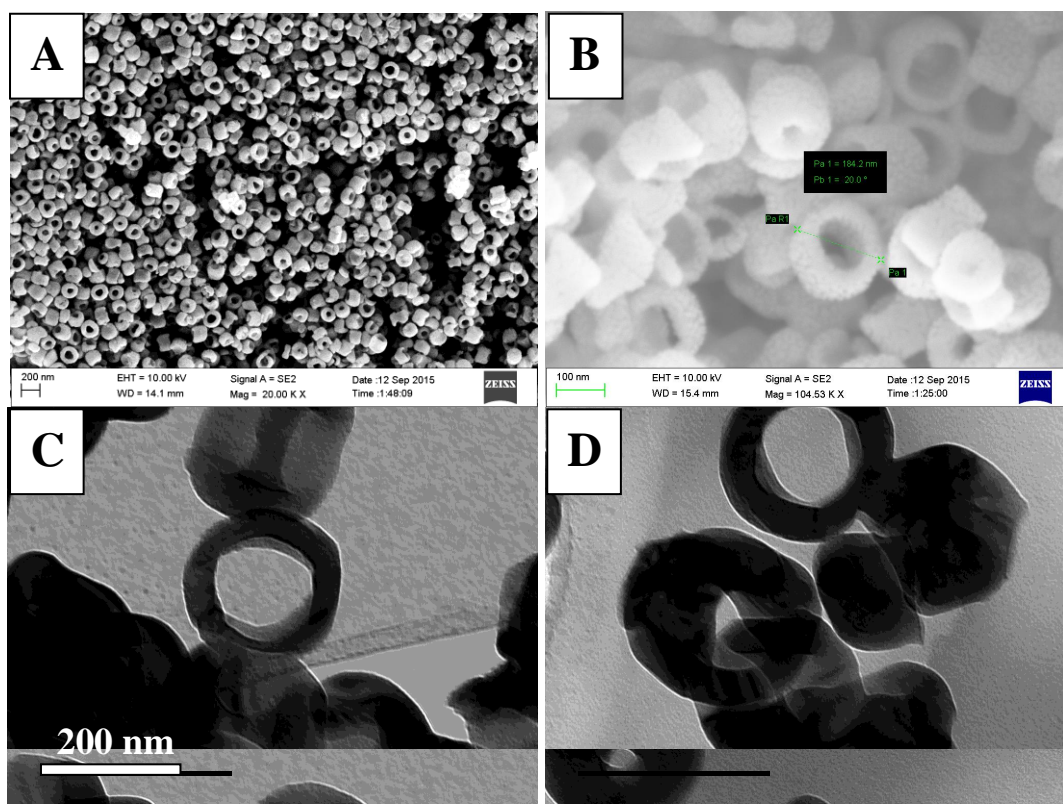


**Figure 1.** SEM (A, B) and TEM (C, D) images of  $\text{Fe}_3\text{O}_4$  NRs.

Figure 1 shows the prepared  $\text{Fe}_3\text{O}_4$  NRs by hydrothermal method. As can be seen in Figure 1, the  $\text{Fe}_3\text{O}_4$  NRs exhibit uniform size and morphology with outer diameters of 160-180 nm, inner diameters of 80-110 nm, and heights of 70-110 nm, indicating the  $\text{Fe}_3\text{O}_4$  NRs have been successfully prepared.

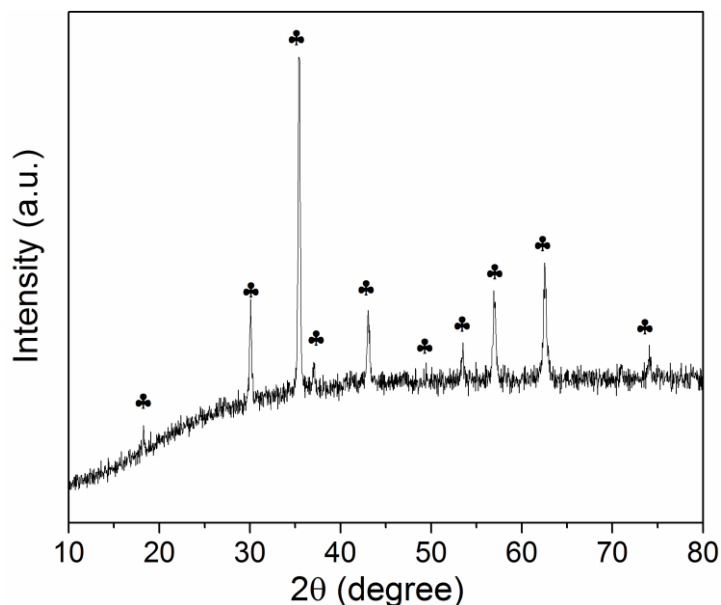


**Figure 2.** XRD patterns of  $\text{Fe}_3\text{O}_4$  NRs.

Figure 2 displays the XRD patterns of as-prepared  $\text{Fe}_3\text{O}_4$  NRs. The diffraction peaks at  $18.3^\circ$ ,  $30.1^\circ$ ,  $35.4^\circ$ ,  $37.1^\circ$ ,  $43.1^\circ$ ,  $47.1^\circ$ ,  $53.4^\circ$ ,  $56.9^\circ$  and  $62.5^\circ$  can be assigned to the (111), (220), (311), (222), (400), (331), (442), (511) and (440) crystal planes of  $\text{Fe}_3\text{O}_4$ , respectively (JCPDS Card No. 87-2334).

+

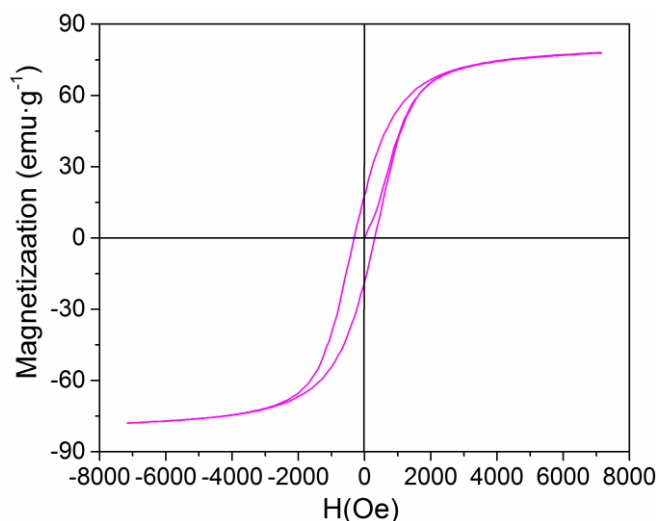


**Figure 3.** Hysteresis loop of  $\text{Fe}_3\text{O}_4$  NRs measured at 300 K.

Figure 3 shows of the magnetization of as-prepared  $\text{Fe}_3\text{O}_4$  NRs. The coercivity of these  $\text{Fe}_3\text{O}_4$  NRs are 120 Oe. The saturation magnetization ( $M_s$ ) of the  $\text{Fe}_3\text{O}_4$  NRs is about 86.2 emu/g, which is smaller than the bulk  $\text{Fe}_3\text{O}_4$  (92 emu/g) [15], because of the decreasing of the particle size. Two kinks near zero magnetization appeared in the  $M$ - $H$  loop, indicating the possibility of an opposite direction of the two vortex states [14].

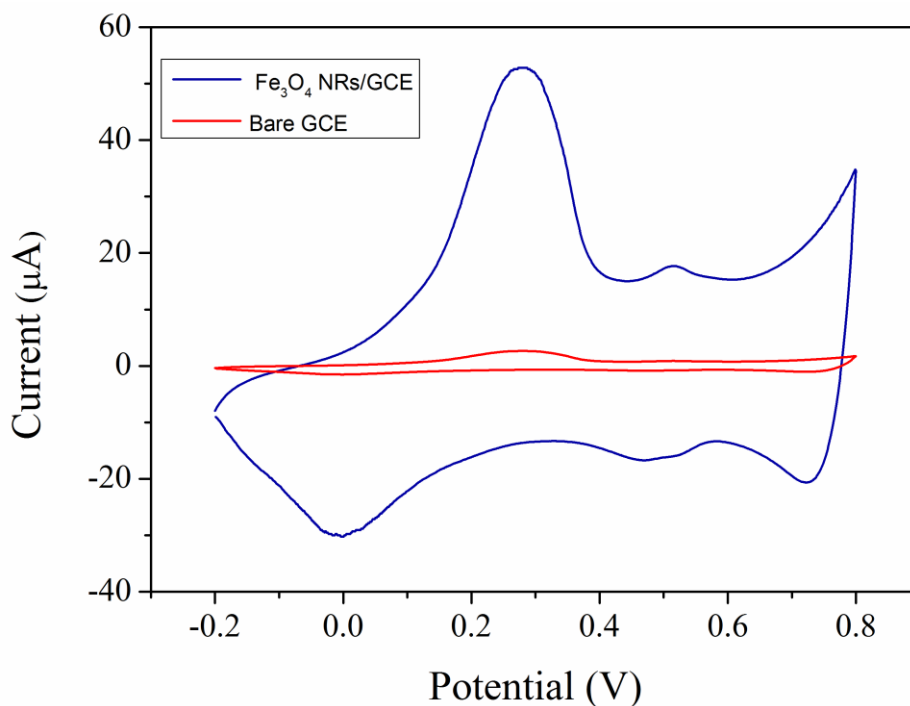


**Figure 4.** CV results of bare GCE and  $\text{Fe}_3\text{O}_4$  NRs/GCE with 1 mM DA in PBS (0.1M, pH 5.0) at scan rate of  $20 \text{ mV s}^{-1}$ .

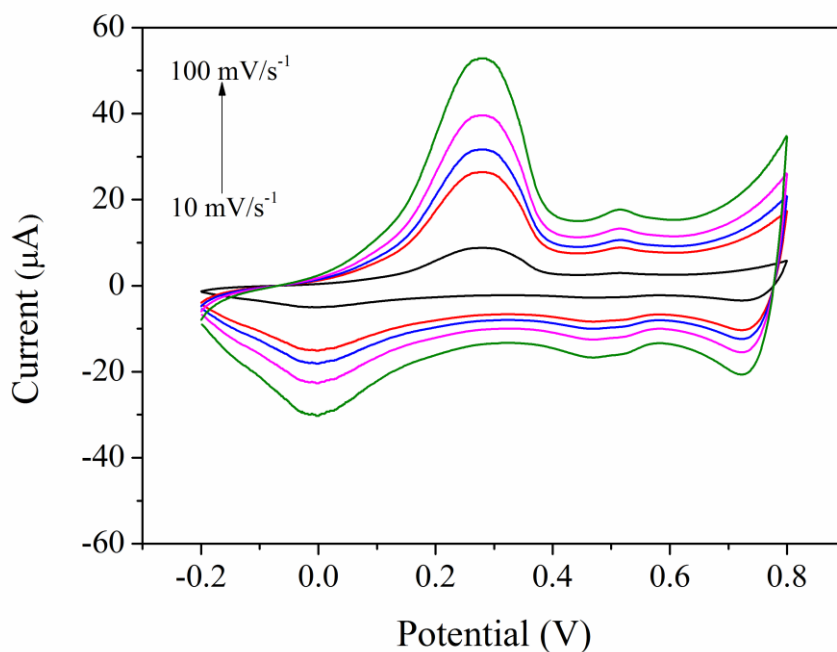


**Figure 5.** CV results of 0.1 mM DA in 0.1 M PBS at the  $\text{Fe}_3\text{O}_4$  NRs at scan rate of  $10\text{-}100 \text{ mV s}^{-1}$ .

To investigate the application of  $\text{Fe}_3\text{O}_4$  NRs, the electrochemical properties in the presence of DA were detected on the  $\text{Fe}_3\text{O}_4$  NRs/GCE. The electrochemical sensing characteristics of bare GCE and  $\text{Fe}_3\text{O}_4$  NRs/GCE electrode were analyzed in PBS as a redox probe at a rate of  $20 \text{ mV/s}$ .

Figure 4 depicts the typical CV responses of 1 mM DA on the bare GCE and the  $\text{Fe}_3\text{O}_4$  NRs/GCE

NRs/GCE. At the bare GCE, DA has a reversible electrochemical behavior and minimal small current, indicating that it detects DA inefficiency. After functionalized with  $\text{Fe}_3\text{O}_4$  NRs, a couple of small redox peaks was observed [16], due to DA is easily oxidized to form dopaminequinone (DAQ) after exchange of 2 electrons and 2 protons [17].

To study the influence of the scan rate on the oxidation current of 0.1 mM DA, the  $\text{Fe}_3\text{O}_4$  NRs/GCE electrode was applied in 0.1 M PBS (pH 5.5) by varying the scan rates from 10 to 100  $\text{mV s}^{-1}$ . As can be seen in Figure 5, with the increasing of the scan rate, the anodic peak currents are risen and moved to more positive positions. In contrast, the cathodic peak currents are slightly moved to more negative positions. These results indicate that the electron transfer rate of  $\text{Fe}_3\text{O}_4$  NRs/GCE electrode decreased, and the electrochemical performance of DA tended to be less reversible [18].

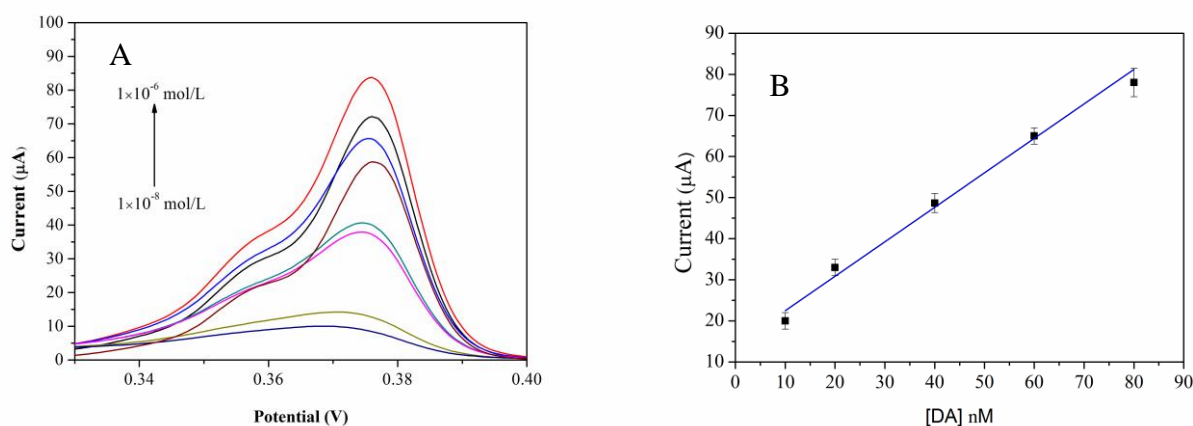


**Figure 6.** DPV results of different DA concentration for  $\text{Fe}_3\text{O}_4$  NRs/GCE based biosensor.

To prove the sensitivity of the  $\text{Fe}_3\text{O}_4$  NRs/GCE based biosensor, DPV was utilized to show the detection of DA. As can be seen in Figure 6, with the DA concentration increasing, the oxidation peak current ( $I_{pa}$ ) rising relatively.

Furthermore, the peak current and DA concentration show linearly proportional in the range from  $1.0 \times 10^{-8}$  to  $1.0 \times 10^{-6}$  M (see Figure 6 (B)). The linear regression equations for DA is  $I(\mu\text{A}) = 14.3 + 0.839 C (10^{-8} \text{ M})$ . The limit for DA detection was conformed to be  $8.67 \times 10^{-9}$  M, which is comparable with other reports [19, 20].

**Table 1.** Comparison of measurement results of the analytical performance with standard and previous measurement methods.

Modified materials	Linear ranges (M)	Detection limits (M)	reference
GO	$1.5 \times 10^{-7}$ to $1 \times 10^{-6}$	$0.27 \times 10^{-6}$	21
Meso-SiO <sub>2</sub> /CPE	$4 \times 10^{-6}$ to $5.2 \times 10^{-5}$	$1.00 \times 10^{-7}$	22
$\text{Fe}_3\text{O}_4/\text{r-GO}$	$4 \times 10^{-7}$ to $1.6 \times 10^{-4}$	$8.00 \times 10^{-8}$	23
HPLC	$2.6 \times 10^{-6}$ to $2.55 \times 10^{-5}$	$2.50 \times 10^{-6}$	24
$\text{Fe}_3\text{O}_4$ NRs/GCE	$1.0 \times 10^{-8}$ to $1.0 \times 10^{-6}$ M	$8.67 \times 10^{-9}$	This work

Table 1 shows the comparison of measurement results of the analytical performance Fe<sub>3</sub>O<sub>4</sub> NRs/GCE with standard high-performance liquid chromatography (HPLC) method and other dopamine detection methods reported recently. Based on the results, the Fe<sub>3</sub>O<sub>4</sub> NRs/GCE biosensor in this work has comparable and even better performance than the standard HPLC method and others, indicating that Fe<sub>3</sub>O<sub>4</sub> NRs/GCE electrode based biosensor has extraordinary potential for DA detection.

**Table 2.** Determination results of DA in real urine samples (n=3).

Detected (μM)	Added (μM)	Found (μM)	RSD (%)	Recovery (%)
0	5.00	5.05±0.12	2.4%	102.4
5.00	10.0	14.92±0.27	1.8%	101.1
10.0	20.0	29.82±0.47	2.2%	101.2

Table 2 summarized the reliability of the Fe<sub>3</sub>O<sub>4</sub> NRs/GCE electrode based detection results of the real human urine samples. In the experiment, the human urines were diluted 5 times with 0.10 M PBS (pH 6.0) before characterization. Then different amounts of DA were added into the sample to test recoveries. The recovery of the spiked samples ranged between 101.1% and 102.4%. Hence, the Fe<sub>3</sub>O<sub>4</sub> NRs/GCE electrode based detection method can be applied to real biological samples in the determination, and obtain satisfactory results.

#### 4. CONCLUSION

In conclusion, we have successfully prepared Fe<sub>3</sub>O<sub>4</sub> NRs *via* a low cost and simple method. The Fe<sub>3</sub>O<sub>4</sub> NRs/GCE electrode was applied as electrochemical biosensor for DA detection, showing excellent electrocatalytic activity and electron transfer rate in the oxidation of DA. Furthermore, compared with the similar DA detection biosensor, the Fe<sub>3</sub>O<sub>4</sub> NRs/GCE electrode exhibited higher sensitivity, selectivity and lower detection limit. These results reveal that Fe<sub>3</sub>O<sub>4</sub> NRs/GCE electrode could be a potential candidate as electrochemical and biological sensors.

#### ACKNOWLEDGEMENTS

This work was supported by The Scientific Research Fund of Mianyang city (14S-01-2), Fundamental Science on Nuclear Wastes and Environmental Safety Laboratory (15kffk05), National Natural Science Foundation of China (31400811), and the Fundamental Research Funds of China West Normal University (14C005).

#### References

1. L. Reverté, B. Prieto-Simón and M. Campàs, *Anal. Chim. Acta.*, 908 (2016) 8-21.
2. J.I. A. Rashid, N.A. Yusof, J. Abdullah, U. Hashim and R. Hajian, *J. Mater. Sci.*, 51 (2016) 1083-1097.
3. Y. Zhou, H. Yin, J. Li, B. Li, X. Li, S. Ai and X. Zhang, *Biosens. Bioelectron.*, 79 (2016) 79-85.



4. W. Wei, P. Ma, D. Hui, H.J. Krause, Z. Yi, D. Willbold, A. Offenhaeusser and Z. Gu, *Biosens. Bioelectron.*, 80 (2016) 661–665.
5. M.E. Cortina, L.J. Melli, M. Roberti, M. Mass, G. Longinotti, S. Tropea, P. Lloret, D.A. Serantes, F. Salomón and M. Lloret, *Biosens. Bioelectron.*, 80 (2016) 24-33.
6. D. Wu, Y. Wang, Y. Zhang, H. Ma, X. Pang, L. Hu, B. Du and Q. Wei, *Biosens. Bioelectron.*, 82 (2016) 9-13.
7. B. Feng and Y.N. Liu, *Int. J. Electrochem. Sci.*, 10 (2015) 4770-4778.
8. O. Galović, M. Samardžić and M. Sak-Bosnar, *Int. J. Electrochem. Sci.*, 10 (2015) 5176-5193.
9. L. Liu, N. Xia, J.J. Meng, B.B. Zhou and S.J. Li, *J. Electroanal. Chem.*, 775 (2016) 58–63.
10. A. Azadbakht, M. Roushani, A. R. Abbasi and Z. Derikvand, *Anal. Biochem.*, 507 (2016) 47–57.
11. Y. Wang, C. Hou, Y. Zhang and M. Liu, *Rsc Adv.*, 5 (2015) 98260-98268.
12. T. Peiksee, A. Pandikumar, H. Nayming, L. Hongnggee and Y. Sulaiman, *Sensors*, 14 (2014) 15227-15243.
13. W. Zhang, J. Zheng, J. Shi, Z. Lin, Q. Huang, H. Zhang, C. Wei, J. Chen, S. Hu and A. Hao, *Anal. Chim. Acta*, 853 (2015) 285–290.
14. C.J. Jia, L.D. Sun, F. Luo, X.D. Han, L.J. Heyderman, Z.G. Yan, C.H. Yan, K. Zheng, Z. Zhang and M. Takano, *J. Am. Chem. Soc.*, 130 (2008) 16968-16977.
15. Q.A. Pankhurst, J. Connolly, S.K. Jones and J. Dobson, *J. Phys. D Appl. Phys.*, 36 (2003) R167-R181.
16. Y. Li, Y. Jiang, T. Mo, H. Zhou, Y. Li and S. Li, *J. Electroanal. Chem.*, 767 (2016) 84-90.
17. S. Palanisamy, X. Zhang and T. He, *J. Mater. Chem. B*, 3 (2015) 6019-6025.
18. W. Dan, Y. Li, Z. Yong, P. Wang, W. Qin and B. Du, *Electrochim. Acta*, 116 (2014) 244-249.
19. T. Peiksee, A. Pandikumar, N.M. Huang, L. Hongnggee and Y. Sulaiman, *Sensors*, 14 (2014) 15227-15243.
20. Z. Terzopoulou, G. Kyzas and D. Bikiaris, *Materials*, 8 (2015) 652-683.
21. F. Gao, X. Cai, X. Wang, C. Gao, S. Liu, F. Gao and Q. Wang, *Sens. Actuators, B*, 186 (2013) 380-387.
22. D. Sun, X.F. Xie, H.J. Zhang, *Colloids Surf. B*, 75 (2010) 88-92.
23. H. Teymourian, A. Salimi and S. Khezrian, *Biosens. Bioelectron.*, 49 (2013) 1-8.
24. V. Sirisha, C. Sreedhar and T. Sreenivasa Rao, *Open Access Sci. Rep.*, 2 (2013) 1-4.